1 *Article - discoveries*

2

3 *Seascape genomics reveals candidate*

4 *molecular targets of heat stress adaptation in*

5 *three coral species*

6

7 Oliver Selmoni[1,2], Gaël Lecellier[2,3], Hélène Magalon[4],

8 Laurent Vigliola[2], Francesca Benzoni[5],

9 Christophe Peignon[2], Stéphane Joost[1],

10 Véronique Berteaux-Lecellier[2]

11
12 1 - Laboratory of geographic information systems, Ecole Polytechnique Federale de Lausanne, Lausanne
13 Switzerland
14 2 - UMR250/9220 ENTROPIE IRD-CNRS-Ifremer-UNC-UR, Labex CORAIL, Nouméa, New Caledonia
15 3 - UVSQ, Université de Paris-Saclay, Versailles, France
16 4 - UMR250/9220 ENTROPIE IRD-CNRS-Ifremer-UNC-UR, Labex CORAIL, Université de La Réunion, St Denis,
17 France
18 5 - Red Sea Research Center, Division of Biological and Environmental Science and Engineering, King Abdullah
19 University of Science and Technology, Thuwal, Saudi Arabia

20

21

22

23 **Corresponding author:**

24 Véronique Berteaux-Lecellier

25 veronique.berteaux-lecellier@ird.fr

26

27

28 **Abstract**

29

30   Anomalous heat waves are causing a major decline of hard corals around the world and

31   threatening the persistence of coral reefs. There are, however, reefs that had been exposed

32   to recurrent thermal stress over the years and whose corals appeared tolerant against heat.

33   One of the mechanisms that could explain this phenomenon is local adaptation, but the

34   underlying molecular mechanisms are poorly known.

35   In this work, we applied a seascape genomics approach to study heat stress adaptation in

36   three coral species of New Caledonia (southwestern Pacific) and to uncover molecular actors

37   potentially involved. We used remote sensing data to characterize the environmental trends

38   across the reef system, and sampled corals living at the most contrasted sites. These samples

39   underwent next generation sequencing to reveal single-nucleotide-polymorphisms (SNPs) of

40   which frequencies associated with heat stress gradients. As these SNPs might underpin an

41   adaptive role, we characterized the functional roles of the genes located in their genomic

42   neighborhood.

43   In each of the studied species, we found heat stress associated SNPs notably located in

44   proximity of genes coding for well-established actors of the cellular responses against heat.

45   Among these, we can mention proteins involved in DNA damage-repair, protein folding,

46   oxidative stress homeostasis, inflammatory and apoptotic pathways. In some cases, the same

47   putative molecular targets of heat stress adaptation recurred among species.

48   Together, these results underscore the relevance and the power of the seascape genomics

49   approach for the discovery of adaptive traits that could allow corals to persist across wider

50   thermal ranges.

51

52

53   **Introduction**

54

55   One of the most dramatic consequences of climate change is the worldwide decline of coral

56   reefs, which are the most biodiverse ecosystems in the marine environment (Hughes et al.

57   2017). Among the main drivers of this decline is coral bleaching, a stress response to

58   anomalous heat waves that eventually causes the death of hard corals (Bellwood et al. 2004;

59   Hughes et al. 2017). In the most severe episodes, coral bleaching provoked local living coral

60   cover loss of up to 50% (Hughes et al. 2017; Hughes et al. 2018), with climate change

61   projections expecting for bleaching conditions to be persistent worldwide by 2050 (Van

62   Hooidonk et al. 2013).

63   Despite these catastrophic perspectives, a glimpse of hope is brought by coral reefs that show

64   resistance after recurrent heat waves (Thompson and van Woesik 2009; Penin et al. 2013;

65   Krueger et al. 2017; Dance 2019; Hughes et al. 2019). One of the mechanisms that might

66   promote heat tolerance in corals is genetic adaptation (Sully et al. 2019). In recent years,

67   there has been a growing body of literature investigating how coral thermal adaptation might

68   alter the predictions of reef persistence, and how conservation policies could be modified

69   accordingly (Logan et al. 2014; Van Oppen et al. 2015; Matz et al. 2018).

70   Given the crucial role adaptation will play in long-term reef persistence, there is an urgent

71   need to characterize the adaptive potential of corals (Logan et al. 2014; Van Oppen et al.

72   2015). For instance, there are still open questions concerning the spatial and temporal scales

73   at which local adaptation operates (Matz et al. 2018; Roche et al. 2018). Changes in adaptive

74   potential have been observed along thermal gradients over hundreds of kilometres (*e.g.*

75   (Thomas et al. 2017), but also at reefs with distinct thermal variations located only a few

76   hundreds of meters apart (*e.g.* Bay and Palumbi 2014). Furthermore, different coral species

77   are reported to show differential vulnerability against thermal stress, leading to the question

78   of how different life-history traits (*e.g.* reproductive strategies) drive the pace of adaptation

79   (Loya et al. 2001; Darling et al. 2012; Hughes et al. 2018).

80   There are also open questions concerning the molecular mechanisms that might be targeted

81   by heat stress adaptation in corals (van Oppen and Lough 2009; Mydlarz et al. 2010; Palumbi

82   et al. 2014). Some cellular responses to heat stress are now well characterized, such as DNA

83   repair mechanisms, the activation of the protein folding machinery in the endoplasmic

84   reticulum (ER) or the accumulation of reactive oxygen species (ROS, either endogenous or

3

85   produced by the symbiont) that progressively elicits inflammatory and apoptotic responses

86   (van Oppen and Lough 2009; Mydlarz et al. 2010; Maor-Landaw and Levy 2016; Oakley et al.

87   2017; Patel et al. 2018). However, little is known about which of the many molecular actors

88   participating to these cascades could be hijacked by evolutionary processes to increment

89   thermal tolerance.

90   Seascape genomics could contribute to filling these gaps. Seascape genomics is a budding

91   field of population genomics that allows the study of local adaptation in wild populations

92   (Riginos et al. 2016). This method combines the environmental characterization of the

93   seascape with a genomic analysis of its population (Rellstab et al. 2015). The goal is to identify

94   genetic variants that correlate with environmental gradients that might underpin an adaptive

95   role (Rellstab et al. 2015). Seascape genomics could enhance the characterization of coral

96   adaptive potential because: (1) it requires an extensive sampling strategy that allows for

97   studying adaptation at different geographic scales, and against different types of

98   environmental constraints simultaneously (*e.g.* mean temperatures, standard deviations,

99   accumulated heat stress; Leempoel et al. 2017; Selmoni et al. 2020a); (2) its experimental

100   protocol is less laborious in comparison to traditional approaches used for studying coral

101   adaptation (*e.g.* aquarium experiments, transplantations), and therefore facilitates scaling-

102   up to a multiple species analysis; (3) it is based on genomic data and thus reports candidate

103   molecular targets of adaptation (Rellstab et al. 2015; Riginos et al. 2016). Moreover, recent

104   work described how the results of seascape genomics studies on corals can be directly

105   transposed to a conservation perspective and support reef prioritization (Selmoni et al.

106   2020b).

107   Here we applied the seascape genomics approach to study the adaptive potential against heat

108   stress in three bleaching-prone coral species of New Caledonia, in the southwestern Pacific

109   (Fig. 1). We first used publicly available satellite data to characterize the seascape conditions

110   for over 1,000 km of the reef system. A sampling campaign was then organized to collect

111   colonies at the 20 sites exposed to the most contrasted environmental conditions. The

112   collected   samples   underwent   a   genotype-by-sequencing   (DArT-seq)   genomic

113   characterization, followed by a seascape genomics analysis accounting for the confounding

114   role of demographic structure. This allowed us to uncover single nucleotide polymorphisms

115   (SNPs) associated with heat stress. We then performed the functional annotations of genes

116   surrounding these SNPs and found molecular targets that notably recurred among species

4

117   and that referred to well established heat stress responses in coral cells. Our study lays the

118   foundations for the discovery of adaptive traits that could allow corals to persist across wider

119   thermal ranges.

120

Figure 1. Study area and sampling sites. The 20 sampling sites around Grande Terre, the main island of New Caledonia (South Western Pacific), are shown in yellow. For every sampling site, the number of genotyped individuals per species (*Acropora millepora*: red, *Pocillopora damicornis*: blue, *Pocillopora acuta*: green) are given in the corresponding boxes.

121

122

123   **Results**

124
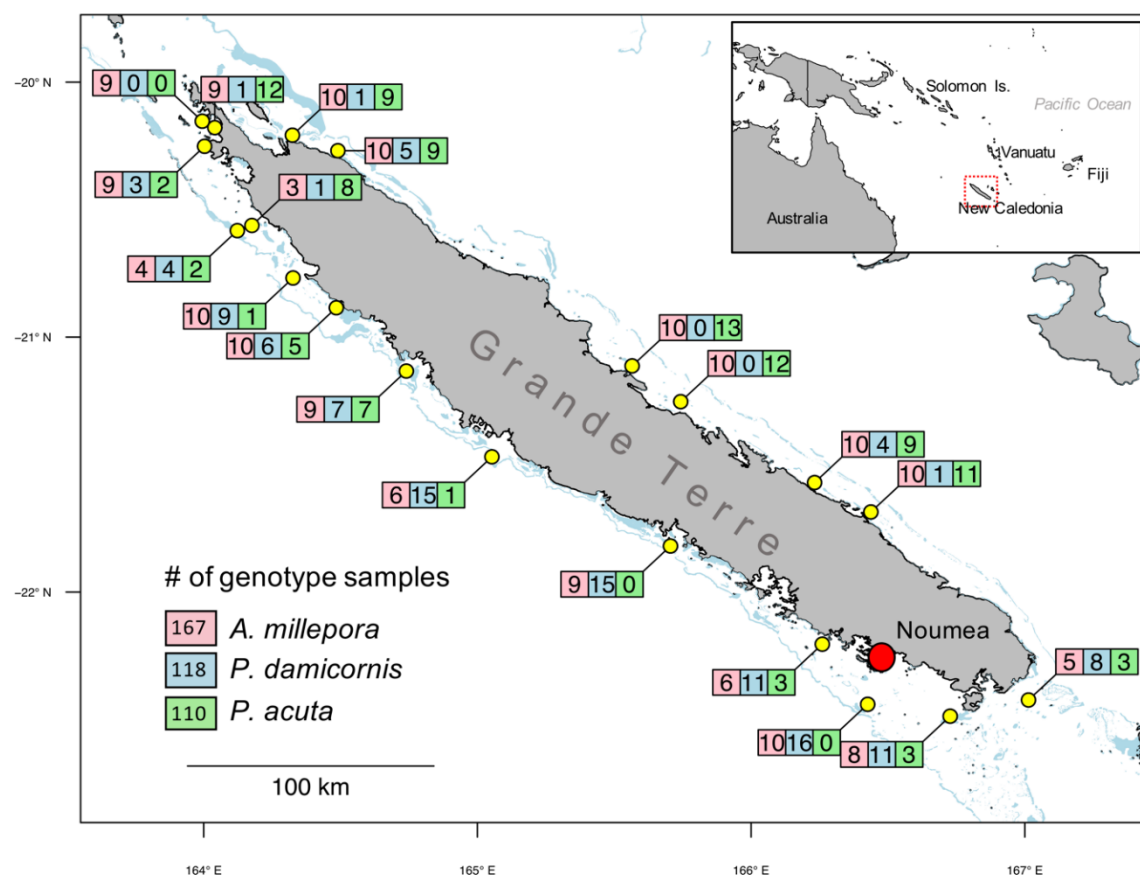
125   Three coral species were sampled at 20 sites across the reef system of New Caledonia:

126   *Acropora millepora* (Ehrenberg, 1834; n=360), *Pocillopora damicornis* (Linnaeus, 1758;

127   (n=128) and *Pocillopora acuta* (Lamarck, 1816 ; n=150; Tab. S2). The DArT-seq analytical

5

128 pipeline resulted in the genotyping of 188 samples by 57,374 bi-allelic single nucleotide

129 polymorphisms (SNPs) for *A. millepora*, and 128 and 150 samples by 70,640 SNPs for

130 *P. damicornis* and *P. acuta*, respectively (Tab. 1)*.* After filtering for rare variants, missing

131 values and clonality, we obtained a final genotype matrix of 167 individuals by 11,935 SNPs

132 for *A. millepora*, of 118 individuals by 7,895 SNPs for *P. damicornis* and of 110 individuals by

133 8,343 SNPs for *P. acuta* (Tab. 1). The *A. millepora* genotyped samples distributed across all

134 the 20 sampling sites (18 of which counted five samples or more), while genotyped samples

135 of *P. damicornis* and *P. acuta* were distributed across 17 sites each (both with 10 sites

136 counting five samples or more), with 15 sites where both species were found in sympatry

137 (Fig. 1; Tab. S1).

Table 1. **Workflow of the analysis.** For each of the species of interest (*Acropora millepora, Pocillopora damicornis, Pocillopora acuta*), we report the number of individuals (ind.) and single nucleotide polymorphism (SNPs) obtained or retained after each the various step of the workflow.

	A. millepora	Pocillopora	
		P. damicornis	P. acuta
Sampling	370 ind.	360 ind.	
Microsatellite	-	128 ind.	150 ind.
DArT-seq	188 ind. x 57,374 SNPs	128 ind. x 70,640 SNPs	150 ind. x 70,640 SNPs
BLAST against reference	188 ind. x 47,529 SNPs	127 ind. x 48,049 SNPs	145 ind. x 48,049 SNPs
Filtering (Missing values, MAF, MGF, LD, clonality)	167 ind. x 11,935 SNPs	118 ind. x 7,895 SNPs	110 ind. x 8,343 SNPs

138

Neutral genetic structure

140

141 We ran a principal component analysis (PCA) of the genotype matrix of each species to

142 anticipate possible confounding role of neutral genomic variation on the adaptation study

143 (Fig. 2, Fig. S1-S2). The Tracy-Widom test (*P*<0.05) revealed that the number of PCs underlying

144 a non-random structure were seven for all the species, accounting for 8% of the total variance

145 in *A. millepora*, 15% in both *P. damicornis* and *P. acuta* (Fig. 2). In *P. damicornis,* the spatial

146 distribution of PC1 values appeared to be spatially structured following a north-south

6

147   separation along the west coast of Grande Terre (Fig. S1B). In *P. acuta,* colonies in the north-

148   west of Grande Terre displayed lower PC1 values, compared to those on the eastern coast

149   (Fig. S1C). In *A. millepora,* no clear geographical patterns emerged as individuals with

150   different values on PC1 were often located on the same reef. Finally, we analysed the

151   presence of genomic widows clustering SNPs with high PC1-loadings, expected to be frequent

152   in genetically isolated groups (cryptic species, hybrids). These genomics windows were rare,

153   as we observed no more than three per species (Fig. S2).

154

Figure 2. Principal component analysis (PCA) of the genotype matrices for three species studied, *Acropora millepora*, *Pocillopora damicornis* and *Pocillopora acuta*. The three graphs display the percentage of variance explained by the first 100 principal components (PC) of the genotype matrix for the three studied species. The vertical dotted lines represent the number of PCs deemed as underlying a non-random structure by the Tracy-Widom test ($P < 0.05$).
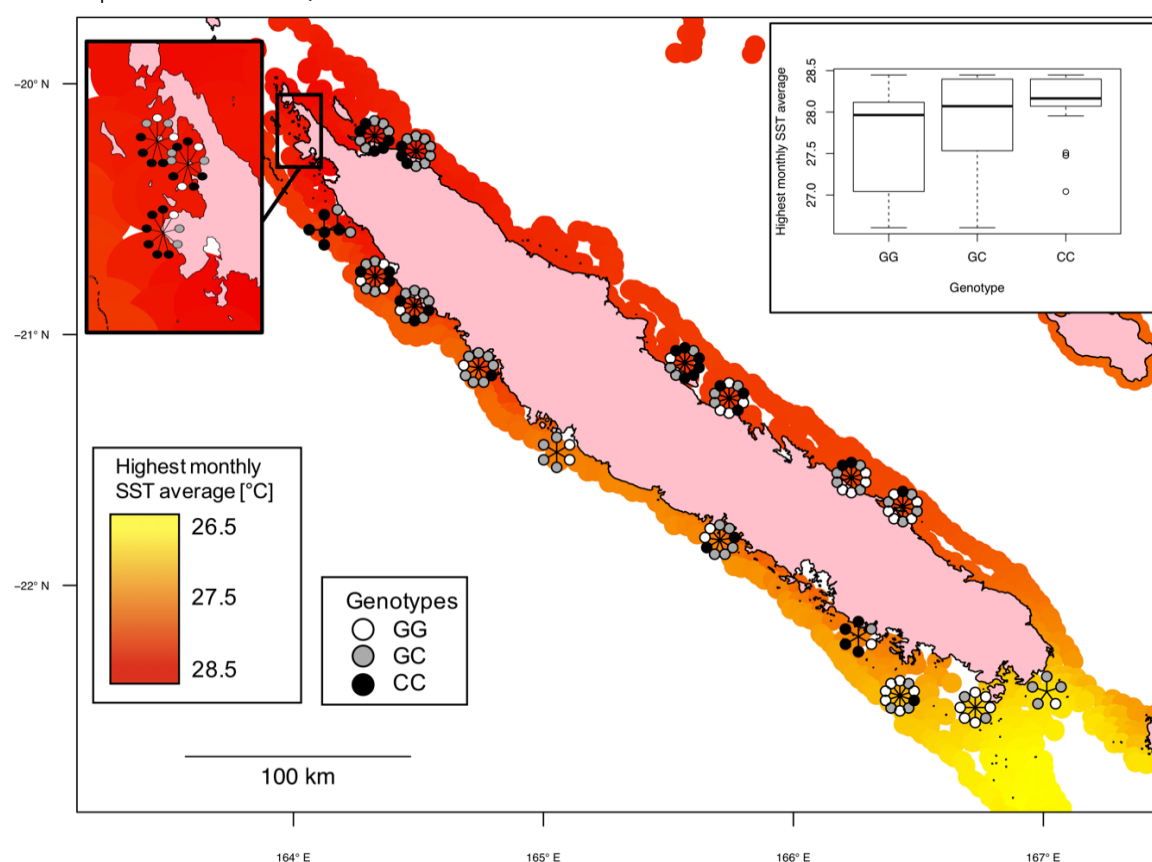

155

156   *Local adaptation*

157
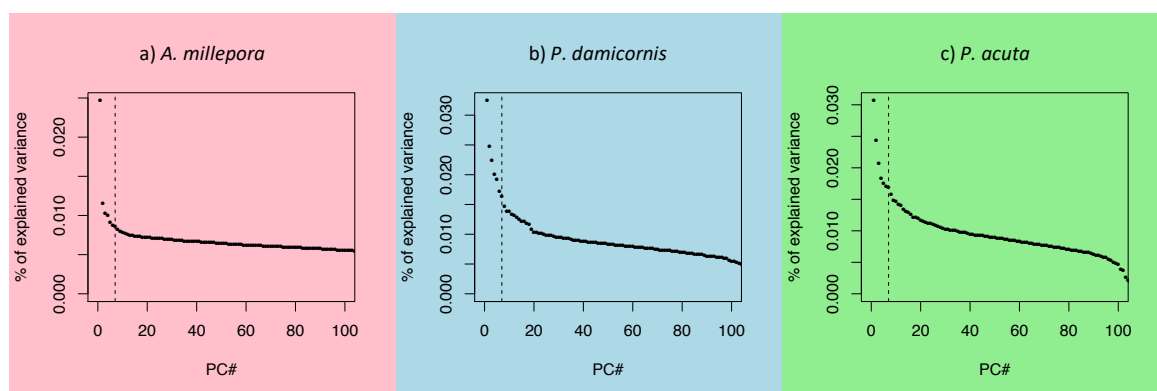
158   We investigated the presence of SNPs that were associated with 47 environmental gradients

159   describing the seascape conditions in New Caledonia (Fig. 3, Fig. S3, Tab. S2). When a SNP was

160   found associated with multiple environmental descriptors, only the most significant

161   association was kept. In total, 120 significant ($q<0.01$) genotype-environment associations

162   were found for *A. millepora*, 90 for *P. damicornis* and 100 for *P. acuta* (Tab. 2a; Tab. S3, S4).

163   In all of the three species, we investigate the environmental descriptors that most frequently

164   associated with significant SNPs were those related to sea surface temperature (SST; 63 in

165   *A. millepora,* 47 in *P. damicornis*, 43 in *P. acuta*). Among these, we found that putative

166   adaptive signals related to bleaching alert frequencies (73 genotype-environment

167   associations) were more frequent than those relating to the standard deviation (42) and

168   average temperatures (38; Tab. 2b).

169   When we focused on the environmental descriptors not relating to temperature, we

170   observed that those describing chlorophyll concentration were those associated to more

171   SNPs (64 across the three species), followed by salinity (40; Tab. 2a). In contrast, current

172   velocity variables were the best environmental descriptors associated with fewer genetic

173   variants (10 across the three species, Tab. 2a).

174

Figure 3. Example of significant genotype-environment association. The map displays the superposition between environmental gradient (here highest monthly SST average) and the distribution of an associated (q<0.01) SNP of *Acropora millepora*. Every circle corresponds to the SNP genotype for an individual colony. For illustrative reasons, genotypes are radially distributed around the sampling locations. The boxplot in the top-right corner shows how the environmental variable distributes within each genotype. The SNP represented here is located on the contig xpSc0000535 (position 118526) of *A. millepora* genome, and the closest annotated gene codes for ATP-dependent DNA helicase Q5.

175

176

Table 2. Significant genotype-environment associations in *Acropora millepora*, *Pocillopora damicornis* and *Pocillopora acuta* Table a displays the number of SNPs significantly associated (*q*<0.01) with environmental descriptors; Table b, the complete list of environmental descriptors related to sea surface temperature (averages and standard deviations at two different spatial resolutions and indices of bleaching alert frequencies - BAF). Note that when a SNP was significantly associate to multiple environmental descriptors, only the best association was kept. The detailed list of the SNP-environment associations is available in the supplementary Table 4.

a)   All environmental descriptors

Environmental descriptor	A. millepora	P. damicornis	P. acuta
Sea surface temperature	63	47	43
Alkalinity	11	7	14
Chlorophyll concentration	15	22	27
Sea current velocity	4	4	2
Suspended particulate matter	8	1	2
Salinity	19	9	12
Total	**120**	**90**	**100**

b)   Sea surface temperature only

Environmental descriptor			A. millepora	P. damicornis	P. acuta
Sea surface temperature	5 km	Overall average	1	0	0
		Average warmest month	1	1	1
		Average coldest month	1	1	0
		Overall standard deviation	1	2	1
		Standard deviation hottest month	0	0	0
		Standard deviation coldest month	11	1	7
		$BAF_{0°C}$	2	1	6
		$BAF_{4°C}$	3	9	1
		$BAF_{8°C}$	1	1	0
		BAF_{CRW}	2	3	0
	1 km	Overall average	0	1	1
		Average warmest month	5	2	4
		Average coldest month	12	4	3
		Overall standard deviation	4	3	2
		Standard deviation hottest month	2	1	0
		Standard deviation coldest month	2	4	1
		$BAF_{0°C}$	10	8	8
		$BAF_{4°C}$	3	3	3
		$BAF_{8°C}$	2	1	1
		BAF_{CRW}	0	1	4
Total			**63**	**47**	**43**

177

Functional annotations of heat stress associated SNPs

179

180   Genes around SNPs that were associated with heat stress were annotated with gene ontology

181   (GO) terms to investigate the molecular functions potentially altered by a genetic variant. GO

182   terms were ranked for over-representation according to the Fisher exact test *P*-value (Tab. 3,

183   S5). Among the top 50 ranks we found GO terms describing molecular functions such as

184   "mismatched DNA binding", "heat shock protein binding", "chaperone binding", "unfolded

185   protein binding", "cytoskeletal protein binding" and "actin binding" in *A. millepora* (Tab. 3a,

9

186   S5a); "actin filament binding receptor activity", "exonuclease activity", "endonuclease

187   activity" and "death effector domain binding" in *P. damicornis* (Tab. 3b, S5b); "NAD binding",

188   "nucleotide binding" and "mitogen-activated protein kinase binding" in *P. acuta* (Tab. 3c,

189   S5c). Four terms ("signaling receptor binding", "receptor regulator activity", "organic cation

190   transmembrane transporter activity", "enzyme activator activity") recurred among top

191   ranked GO terms in at least two different species (Tab. 3). Each of the three species displayed

192   top ranked GO terms referring to "oxidoreductase activity" acting on different molecules

193   (Tab. 3).

194

Table 3. Functional annotations of heat stress associated SNPs. For each of the studied species, *Acropora millepora*, *Pocillopora damicornis* and *Pocillopora acuta,* the tables display the list of GO terms describing molecular functions that are overrepresented in the genomic neighborhoods (± 50 kb) of heat stress associated SNPs. For each GO term, the tables display the id (GO.ID), the term description (Term), the occurrence in the genome split in 100 kb windows (#Ann.), the observed (#Obs.) and expected (#Exp.) occurrence in the neighborhoods of heat stress associated SNPs and the *P*-value associated to the Fisher exact test comparing the expected and observed occurrences. For every species, the tables show a subset of the top 50 GO terms. The complete list of top ranked GO terms is available in the supplementary material (Tab. S5). GO terms in bold are those appearing in the top GO list of two different species.

a) *A. millepora*

Rank	GO.ID	Term	#Ann.	#Obs.	#Exp.	*P*-value
3	GO:0003779	actin binding	278	11	4.25	<0.01
10	GO:0016670	oxidoreductase activity, acting on a sulfur group of donors, oxygen as acceptor	10	2	0.15	0.01
12	GO:0098772	molecular function regulator	724	19	11.07	0.01
15	GO:0008047	**enzyme activator activity**	244	9	3.73	0.01
16	GO:0030547	receptor inhibitor activity	11	2	0.17	0.01
25	GO:0016701	oxidoreductase activity, acting on single donors with incorporation of molecular oxygen	38	3	0.58	0.02
26	GO:0019209	kinase activator activity	39	3	0.6	0.02
32	GO:0030983	mismatched DNA binding	16	2	0.24	0.02
33	GO:0043028	cysteine-type endopeptidase regulator activity involved in apoptotic process	16	2	0.24	0.02
34	GO:0008092	cytoskeletal protein binding	644	16	9.85	0.03
39	GO:0015101	**organic cation transmembrane transporter activity**	19	2	0.29	0.03
41	GO:0051082	unfolded protein binding	83	4	1.27	0.04
43	GO:0060090	molecular adaptor activity	167	6	2.55	0.04
44	GO:0016620	oxidoreductase activity, acting on the aldehyde or oxo group of donors, NAD or NADP as acceptor	22	2	0.34	0.04
47	GO:0031072	heat shock protein binding	88	4	1.35	0.04
50	GO:0030545	**receptor regulator activity**	131	5	2	0.05

b) P. damicornis

Rank	GO.ID	Term	#Ann.	#Obs.	#Exp.	*P*-value
2	GO:0005506	iron ion binding	126	6	1.78	0.01
7	GO:0016705	oxidoreductase activity, acting on paired donors, with incorporation or reduction of molecular oxygen	167	6	2.36	0.03
8	GO:0051015	actin filament binding	127	5	1.79	0.03
11	GO:0048487	beta-tubulin binding	24	2	0.34	0.04
15	GO:0008047	**enzyme activator activity**	251	7	3.55	0.06
17	GO:0004888	transmembrane signaling receptor activity	1045	20	14.76	0.06
19	GO:0008528	G protein-coupled peptide receptor activity	324	8	4.58	0.08
20	GO:0005102	**signaling receptor binding**	749	15	10.58	0.08
30	GO:0005096	GTPase activator activity	139	4	1.96	0.13
40	GO:0038023	signaling receptor activity	1142	20	16.13	0.14
42	GO:0016796	exonuclease activity, active with either ribo- or deoxyribonucleic acids and producing 5'-phosphomonoesters	47	2	0.66	0.14
46	GO:0016894	endonuclease activity, active with either ribo- or deoxyribonucleic acids and producing 3'-phosphomonoesters	11	1	0.16	0.15
47	GO:0030169	low-density lipoprotein particle binding	11	1	0.16	0.15
49	GO:0035877	death effector domain binding	11	1	0.16	0.15

c) P. acuta

Rank	GO.ID	Term	#Ann.	#Obs.	#Exp.	*P*-value
5	GO:0022857	transmembrane transporter activity	702	18	10.17	0.01
9	GO:0015368	calcium:cation antiporter activity	11	2	0.16	0.01
10	GO:0005102	**signaling receptor binding**	749	18	10.85	0.01
21	GO:0015101	**organic cation transmembrane transporter activity**	16	2	0.23	0.02
35	GO:0000166	nucleotide binding	1297	25	18.79	0.03
41	GO:0031435	mitogen-activated protein kinase binding	23	2	0.33	0.04
42	GO:0030545	**receptor regulator activity**	137	5	1.98	0.05
45	GO:0051287	NAD binding	57	3	0.83	0.05
47	GO:0016651	oxidoreductase activity, acting on NAD(P)H	59	3	0.85	0.05
49	GO:0090722	receptor-receptor interaction	26	2	0.38	0.05

195

196

Discussion

Different types of heat stress adaptation

In each of the studied species, we detected genotype-environment associations that might underpin local adaptation (Tab. 2a). Approximately half of these associations concerned descriptors of sea surface temperature (SST; Tab. 2a), partially because these are the most numerous types of descriptors employed in the analysis (20 out of 47; Tab. S2a).

As we focused on SST-related associations, we found that those involving bleaching alert frequencies (BAFs) were more frequent (73) than those related to temperature variations (42) and temperature averages (38; Tab. 2). Coral bleaching is a major threat for coral survival, and bleaching conditions emerge when SST variation exceeds seasonal averages (Liu et al. 2003; Hughes et al. 2017). BAFs descriptors account precisely for this selective constraint (SST variation over average), and this might explain why genotype-environment associations with BAFs were more frequent. Previous work on coral seascape genomics also reported a predominance of adaptive signals related to BAF (Selmoni et al. 2020b). Coral adaptation appeared to be also driven by SST averages (regardless of variations) or by SST variations (regardless of the averages; Tab. 2b). This kind of adaptation might relate to bleaching (*e.g.* being adapted to high thermal variability promotes bleaching resistance; Safaie et al. 2018), or to other types of heat stress responses (*e.g.* impaired injury recovery at elevated average SST; Bonesso et al. 2017).

Candidate molecular targets for heat stress adaptation

Previous research reported that reefs exposed to high frequency of daily thermal variability showed reduced bleaching prevalence (Safaie et al. 2018). One of the reasons might be that corals at these sites manage to rapidly readjust their cellular homeostasis (Ruiz-Jones and Palumbi 2017). This view is supported by the numerous GO terms describing activity regulators (for instance "signaling receptor binding", "receptor regulator activity", "enzyme activator activity", "molecular function regulator"; Tab. 3, S5) found surrounding heat stress associated SNPs. The fact that these terms are not heat stress specific, however, invites to a cautious interpretation.

229 In contrast, we also detected several genes coding for well-established molecular actors of

230 corals thermal stress responses in the neighborhood of heat stress associated SNPs (Tab. 4,

231 S4). In some rare cases, we found that SNPs fell directly in the coding sequence of genes, but

232 more frequently the SNPs were located several kb distance from genes (Tab. 4). However, this

233 does not exclude causative effects, as (1) the SNP detected could be physically linked to an

234 adaptive SNP in the coding sequence; (2) the adaptive SNP could be located several kb from

235 the target gene, as it is often the case (Brodie et al. 2016). Hereunder, we highlight the

236 different molecular functions and the related proteins that were found as potential targets

237 for thermal adaptation in corals.

238

239 *- DNA repair*

240 Heat stress impacts the integrity of nucleic acids and elicits mechanisms that promote DNA

241 damage-repair and RNA stability (Henry et al. 1992; Sottile and Nadin 2018). A previous

242 seascape genomics study on *Acropora digitifera* found five SNPs associated with heat stress

243 to be proximal to genes coding for Helicase Q (Selmoni et al. 2020b). Here we found Helicase

244 Q5 in the genomic neighbourhood of a SNP associated with heat stress in *A. millepora*

245 (Tab. 4). Helicases Q are required for efficient DNA repair during the initiation of the

246 replication fork (Sharma et al. 2006). Another family of helicases participating to this process

247 are Helicases MCMs (Daniel et al. 2013) and one was found next to an heat stress associated

248 SNP in *A. millepora* (Fig.3; Tab. 4).

249 In addition, we found proteins involved in DNA damage-repair that are known to be

250 differentially expressed in corals under heat stress. For instance, claspin (Palumbi et al. 2014;

251 Smits et al. 2019) and RAD51/54 homologs (Maor-Landaw and Levy 2016) were found here

252 surrounding heat stress associated SNPs in *A. millepora*, while DNA damage-binding protein 1

253 (Li et al. 2006) and DNA polymerase delta catalytic subunit (Prindle and Loeb 2012) in

254 *P. damicornis* (Tab. 4). Of note, GO terms describing molecular functions related to DNA

255 repair ("mismatched DNA binding", "exonuclase activity", "endonuclease activity",

256 "nucleotide binding") were found as over-represented in genes surrounding heat stress

257 associated SNPs in the three species (Tab. 3).

258

259 *- Protein folding*

13

260   One of the main groups of gene annotations surrounding heat stress associated SNPs

261   concerned molecular chaperones (Tab. 4). These are proteins that intervene in cellular

262   responses to heat stress, where they assist the folding or unfolding of proteins in the

263   endoplasmic reticulum notably (ER; Oakley et al. 2017). In corals, the role of these proteins in

264   heat response, as well as their up-regulation under thermal stress, have been reported in

265   several studies (Desalvo et al. 2008; Ishikawa et al. 2009; van Oppen and Lough 2009; Desalvo

266   et al. 2010; Rosic et al. 2011; Maor-Landaw and Levy 2016; Oakley et al. 2017; Ruiz-Jones and

267   Palumbi 2017). The annotation analysis for the related GO terms (*e.g.* "heat shock protein

268   binding", "unfolded protein binding"), revealed that this function was over-represented in

269   genes close to the heat stress associated SNPs of *A. millepora* (Tab. 3a). In the three species,

270   the genomic neighborhood of heat stress associated SNP contained several classes of

271   chaperones: DnaJ homologs (four in *A. millepora,* one in *P. damicornis*), Tubulin-specific

272   chaperone A and NudC domain-containing protein (*A. millepora*; Zheng et al. 2011), prolyl 3-

273   hydroxylase 1 (*P. damicornis*; Ishikawa et al. 2009) and selenoprotein-F (*P. acuta;* Ren et al.

274   2018)*.* Another important class of chaperones are "Protein disulfide-isomerase", which

275   catalyze the formation or breakage of disulfide bonds in proteins and produce reactive oxygen

276   species (ROS) as byproducts (van Oppen and Lough 2009; Oakley et al. 2017). For example,

277   the disulfide-isomerase gene expression has been shown to be upregulated in *Stylophora*

278   *pistillata* under experimental heat stress (Maor-Landaw et al. 2014). Disulfide-isomerase 2

279   genes were found next to heat stress associated SNPs in each of the studied species (Tab. 4).

280

281   *- Oxidative stress response*

282   In parallel to the protein folding and recycling response, coral cells under heat stress

283   accumulate ROS (Oakley et al. 2017; Nielsen et al. 2018). This accumulation can derive from

284   the leakage of ROS from the damaged photosynthetic machinery of the endosymbiont, as

285   well as from the endogenous production of the host mitochondria elicited under heat stress

286   (Oakley et al. 2017; Nielsen et al. 2018). ROS accumulation causes oxidative stress, and the

287   GO terms describing the inherent responses ("oxidoreductase activity") were found as over-

288   represented in genes next to heat stress associated SNPs in the three studied species (Tab. 3).

289   For instance, we found genes coding for Peroxidasin homolog and Isocitrate dehydrogenase

290   subunit beta next to heat stress associated SNPs in *A. millepora* (Tab. 4). Peroxidasin homolog

291   is in the first line of defence against ROS accumulation, displays high rates of evolution in

292   *A. millepora* and was found highly up-regulated under heat stress in *Monstastraea faveolata*

293   (= *Orbicella faveolata*; Voolstra et al. 2009; Voolstra et al. 2011; Louis et al. 2017)*. Isocitrate

294   dehydrogenase is one of the few sources of NADPH in the animal cell and was found

295   upregulated in *E. pallida* under heat stress (Kültz 2005; Oakley et al. 2017). NADPH is an

296   essential substrate to contrast ROS accumulation (Oakley et al. 2017; Patel et al. 2018) and

297   another gene implicated in its metabolism, Quinone oxidoreductase PIG3, was found close to

298   heat stress associated SNPs in *P. acuta* (Tab. 4; Zangar et al. 2004). In *P. damicornis,* we found

299   the Glutathione peroxidase 5 gene, belonging to a family of well-characterized antioxidants

300   contrasting ROS accumulation in corals (Nielsen et al. 2018).

301   In the host mitochondria, ROS production occurs in a series of redox reactions across the inner

302   membrane (the electron transport chain; Lutz et al. 2015). One of the main components of

303   this chain is the respiratory complex I (NADH-ubiquinone oxidoreductase), and we found

304   genes coding for two of its subunits in the genomic neighborhood of heat stress associated

305   SNPs in both *Pocillopora* species (Tab. 4). The mechanism leading to ROS leakage from host

306   mitochondria into coral cell cytoplasm is poorly known (Dunn et al. 2012; Oakley et al. 2017;

307   Nielsen et al. 2018). However, it is noteworthy to mention that in *A. millepora* the SNP most

308   strongly associated with heat stress was close to the MIC60 gene (Tab. 4, S4a). MIC60 is a

309   subunit of the MICOS complex, a key protein in the maintenance of the mitochondrial inner

310   membrane architecture, through which ROS are produced, and the outer membrane, through

311   which ROS diffuse into cytoplasm (Muñoz-Gómez et al. 2015; Zhao et al. 2019).

312

313   - Inflammatory response and apoptosis

314   The effects of ROS depends on the level of accumulation: medium levels elicit an

315   inflammatory response, while excessive levels lead to cell apoptosis (Patel et al. 2018).

316   Mitogen-activated protein kinases (MAPK) are key actors in the inflammatory response (Son

317   et al. 2013; Courtial et al. 2017; Patel et al. 2018). In corals, MAPKs were shown to repress

318   ROS accumulation in *S. pistillata* (Courtial et al. 2017) and were found in proximity of a SNP

319   associated to heat stress in another seascape genomics study on Japanese *A. digitifera*

320   (Selmoni et al. 2020b). Here we found a MAPK coding gene around heat stress associated

321   SNPs in *A. millepora* (MAPK1), and genes coding for a MAPK activating protein *P. damicornis*

322   (Putative MAPK-activating protein FM08) and *P. acuta* (TNF receptor-associated factor 6;

323   Tab. 4; Mason et al. 2004).

15

324   ROS excess eventually results in cell apoptosis (Patel et al. 2018). In each of the three species,

325   we found apoptosis-related genes near heat stress associated SNPs: Programmed cell death

326   protein 6 and Death-associated protein kinase 2 (*A. millepora);* Death effector domain-

327   containing protein (*P. damicornis*); and apoptosis regulator Bcl-2 and Death-associated

328   protein 4 (*P. acuta*; Tab 4). These proteins participate in the caspase-mediated apoptotic

329   cascade involved in the coral bleaching process (Ahmad et al. 1997; Dunn et al. 2007; Valmiki

330   and Ramos 2009; Tchernov et al. 2011; Yuasa et al. 2015; Oakley et al. 2017)*.*

331

332   *- Cell structure*

333   Heat stress has been shown to lead to cytoskeleton reorganization (Wilson et al. 2016). In

334   Cnidaria, cytoskeletal proteins displayed changes in abundance under experimental heat

335   stress in *Exaiptasia pallida* and *A. palmata* (Ricaurte et al. 2016; Oakley et al. 2017). Here we

336   found several genes implicated in the cytoskeletal architecture in proximity of SNPs

337   associated to heat stress: myosin III (twice), unconventional myosin VIIb and actin

338   (*A. millepora*), unconventional myosin-Id (*P. damicornis*), Myosin heavy chain and actin-1

339   (*P. acuta*; Tab. 4). Moreover, the GO terms "actin binding" and "cytoskeletal protein binding"

340   were over-represented in the set of genes neighbouring heat stress associated SNPs in

341   *A. millepora*, and "actin filament binding" in *P. damicornis* (Tab. 3a-b). Of note, in three of the

342   myosin genes the heat stress associate SNPs were found inside the coding sequence (Tab. 4,

343   S4).

344

Table 4. Candidate molecular targets for coral adaptation to heat stress. Annotations of genes surrounding (± 50 kb) heat stress associated SNPs were sorted by molecular function. For six specific types of molecular functions, the table displays the genes potentially involved in heat stress response (Putative molecular target) and the position of the corresponding SNP associated with heat stress (SNP position, in format contig/chromosome: base position). The CDS tag indicates SNP falling inside the coding sequence of the putative molecular target. The background colours correspond to the species where the candidate molecular target was found (pink: *Acropora millepora,* blue: *Pocillopora damicornis,* green: *Pocillopora acuta*). The role that each molecular function has in coral heat response is described in the last column.

Molecular function	SNP position	Putative molecular target	Role in coral heat response
DNA damage repair	xpSc0000535:118526	ATP-dependent DNA helicase Q5	Heat stress and UV radiation can provoke DNA damage. Proteins in this list participate to the DNA damage-repair mechanism during replication.
	chr7:20210292	DNA helicase MCM9	
	chr13:7351849	DNA repair protein RAD51 homolog 2	
	chr13:20841309	Claspin	
	NW_020844825.1:56001	DNA polymerase delta catalytic subunit	
	NW_020847490.1:185714	DNA damage-binding protein 1	
Protein folding / chaperone / heat stress responses	chr7:2529319	DnaJ homolog subfamily B member 6	Molecular chaperones are activated in early response to thermal stress to assist protein folding in the endoplasmic reticulum.
	Sc0000122:685084	Sacsin (DnaJ homolog subfamily C member 29)	
	chr3:18355053		
	chr5:20803650	DnaJ homolog subfamily A member 3	
	chr5:10318559	NudC domain-containing protein 2	
	chr13: 18019180	Tubulin-specific chaperone A	
	chr12:16446416	Protein disulfide-isomerase 2	
	NW_020844635.1:120545	prolyl 3-hydroxylase 1	
	NW_020844967.1:239041	DnaJ homolog subfamily C member 9	
	NW_020845264.1:254233	Protein disulfide-isomerase 2	
	NW_020846699.1:47695	Protein disulfide-isomerase 2	
	NW_020847700.1: 75539	selenoprotein-F	
Oxidative stress	chr2:15023513	MIC60	Heat stress leads to the accumulation of ROS. All the proteins in this list participates to the metabolism of ROS. MIC60 is a key structural protein of the inner membrane of mitochondria were endogenous ROS is produced.
	xfSc0000142:60614	Peroxidasin homolog	
	chr7:20210292	Isocitrate dehydrogenase [NAD] subunit beta	
	NW_020843829.1:322689	NADH-ubiquinone oxidoreductase 23 kDa subunit	
	NW_020844825.1:56001	Glutathione peroxidase 5	
	NW_020846699.1:47695	NADH-ubiquinone oxidoreductase B16.6 subunit	
	NW_020845243.1:143874	Quinone oxidoreductase PIG3	
Inflammatory and apoptotic response	chr13:19271503	Mitogen-activated protein kinase-binding protein 1 (MAPK1)	MAPKs are activated in the inflammatory response caused by ROS accumulation. Excessive ROS accumulation elicits the caspases-mediated apoptotic response observed in coral bleaching.
	chr11:11687264	Death-associated protein kinase 2	
	xfSc0000077:45906	Programmed cell death protein 6	
	NW_020844212.1: 38069 (CDS)	Partial similarity with DED domain-containing protein	
	NW_020845264.1:254233	Putative MAPK-activating protein FM08	
	NW_020846901.1:188731	apoptosis regulator Bcl-2	
	NW_020846154.1:13424	Death-associated protein 4	
	NW_020846522.1:185468	TNF receptor-associated factor 6	
Cytoskeleton	chr1:19795515	Myosin IIIA	ROS accumulation degrade structural proteins and lead to a pronounced reorganization of the cytoskeleton.
	chr12:22835441 (CDS)	Unconventional myosin-VIIb	
	chr2:15023513 (CDS)	Partial similarity with Myosin III	
	chr3:17298197	Actin, cytoplasmic	
	NW_020844967.1:239041	Unconventional myosin-Id	
	NW_020847027.1:161971	Actin-1	
	NW_020846942.1:1165830 (CDS)	Myosin heavy chain	

345

Limitations and future directions

347

348 Seascape genomics studies are exploratory analyses that come with the drawback of being

349 subjected to high false discovery rates (Rellstab et al. 2015; Riginos et al. 2016). This bias is

350 stressed when the confounding role of neutral genetic variation is not accounted for (Selmoni

351 et al. 2020a). The preliminary analysis of population structure, however, did not reveal any

352 cryptic speciation nor isolated reefs among the studied populations (Fig. 2, S1-S2).

353   Furthermore, we used a statistical method (LFMM) and a sampling design allowing to mitigate

354   such confounding effects (Frichot et al. 2013; Selmoni et al. 2020a).

355   There are, nevertheless, some points that could have increased the statistical power of the

356   analysis, as for instance the use of a larger sample size (over 200 individuals per species;

357   (Selmoni et al. 2020a). In addition, the assignment of heat stress associated SNPs to candidate

358   molecular targets for adaptation would have been further facilitated with a higher genome

359   resolution in the sequencing strategy. Higher genome resolution would also allow to infer the

360   structural modification that SNPs falling inside the coding sequence might cause. In the years

361   to come, whole-genome-sequencing on corals is likely to become more affordable and can

362   then be applied to the large sample sizes required for seascape genomics studies.

363   The next step in the characterization of corals' adaptive potential is experimental validation.

364   Our work found several genetic variants that might confer selective advantages against

365   thermal stress (Tab. 4). For each of the studied species, we can now define multiple-loci

366   genotypes of heat stress resistant colonies and test their fitness under experimental heat

367   stress conducted in aquaria (Krueger et al. 2017). As a result, this analysis will allow to 1)

368   further investigate the role of different heat stress associated genotypes and molecular

369   pathways and 2) provide a concrete measure of the thermal ranges that these coral

370   populations might sustain in the years to come. This information is of paramount importance,

371   as it will allow to predict the reefs that are expected to already carry heat tolerant colonies

372   and to define conservation strategies accordingly (Selmoni et al. 2020b). For instance, marine

373   protected areas could be established to preserve reefs with higher adaptive potential against

374   heat stress, where such reefs could provide the breeding stock to restore the damaged ones

375   (Baums 2008; Van Oppen et al. 2015; van Oppen et al. 2017).

376

377   *Conclusions*

378

379   In this study, seascape genomics allowed to uncover genetic variants potentially implicated

380   in adaptive processes against different types of heat stress in three coral species of New

381   Caledonia. These variants were located next to genes coding for molecular actors that

382   participate in well-understood cellular reactions against thermal stress. In addition, the

383   approach pointed out new candidate genes (*e.g.* Helicase Q) or processes (*e.g.* signalling

384   receptor binding) that might be implied in such responses. Of note, some of these potential

385   targets for adaptation recurred in the analyses of different species, supporting the robustness

386   and the power of the seascape genomics. Future studies will focus on performing

387   experimental assays to validate the implication of potentially adaptive genotypes and newly

388   identified genes in the heat stress response and to measure the thermal ranges tolerated by

389   the diverse adaptive genotypes.

390

391

392   **Material and methods**

393

394   *Environmental data*

395

396   The seascape genomics approach requires an exhaustive description of the environmental

397   conditions in order to prevent the misleading effect of collinear gradients (Riginos et al. 2016;

398   Leempoel et al. 2017). For this reason, the seascape characterization we used encompassed

399   seven environmental variables: sea water temperature (SST), chlorophyll concentration, sea

400   surface salinity, sea current velocity, suspended particulate matter, alkalinity and bleaching

401   alert frequencies (BAF; Tab. S2). The environmental characterization was performed in the R

402   environment (R Core Team 2016) using the *raster* package (Hijmans 2016) and following the

403   method described in previous work on coral seascape genomics (Selmoni et al. 2020b) with

404   some modifications outlined hereafter.

405   For the description of SST we used two different georeferenced datasets covering the extent

406   of New Caledonia: (1) daily records of SST since 1981 at a spatial resolution of 5 km (SST_{5km};

407   EU Copernicus Marine Service 2017); (2) daily records of SST since 2002 at resolution of 1 km

408   (SST_{1km}; Group for High Resolution Sea Surface Temperature; Chao et al. 2009; Chin et al.

409   2017). The first dataset covers a wider temporal range, therefore providing a more reliable

410   characterization of historical trends. The second dataset covers a smaller temporal window,

411   but the higher geographic resolution allows to portray fine scale thermal patterns with a

412   higher degree of confidence. Both datasets were used to compute, for each pixel of the study

413   area, averages and standard deviations of the warmest month, the coldest month, and the

414   entire observational period. Furthermore, both datasets were used to compute three indices

415   of bleaching alert frequencies (BAF), representing the frequency of days (over the whole

416   period of remote sensing) during which the bi-weekly accumulated heat stress (*i.e.* SST above

417   the average maximum) exceeded 0°C (BAF$_{0°C}$), 4°C (BAF$_{4°C}$) and 8°C (BAF$_{8°C}$) (Selmoni et al.

418   2020b). Similarly, we computed the frequency of the bleaching warning conditions as defined

419   by the Coral Reef Watch (BAF$_{CRW}$), corresponding to the accumulation of heat over the three

420   previous months (Liu et al. 2003).

421   For the other datasets (chlorophyll concentration, sea surface salinity, sea current velocity

422   and suspended particulate matter; EU Copernicus Marine Service 2017), the spatial resolution

423   ranged between 4 and 9 km (Tab. S2). All the datasets covered a temporal extent of at least

424   20 years before 2018 (the year of sampling) and were processed to compute: (1) highest

425   monthly average, (2) lowest monthly average and (3) overall average. For all the datasets

426   captured at daily resolution (*i.e.* all except suspended particulate matter), we also computed

427   the standard deviation associated with the three means. Seawater alkalinity was estimated

428   by combining SST$_{5km}$ and salinity in a polynomial equation as described by Lee and colleagues

429   (Lee et al. 2006).

430   In total, 47 environmental descriptors (Tab. S2) were computed and assigned to the shapes

431   of the reefs of New Caledonia (UNEP-WCMC et al. 2010), reported for a regular grid (~3,000

432   cells of size: 2x2 km) using QGIS (QGIS development team 2009).

433

434   *Sampling*

435

436   Twenty sampling sites were selected out of the ~3,000 reef cells surrounding Grande Terre,

437   the main island of New Caledonia (Fig. 1). Sampling sites were chosen following an approach

438   that simultaneously maximized environmental contrasts and replicated them at distant sites

439   (the "hybrid approach" described in Selmoni et al. 2020a). The method consists of applying

440   Principal Component Analysis (PCA) and hierarchical clustering to the 47 environmental

441   descriptors in order to separate the ~3,000 reef cells into distinct environmental regions.

442   Next, the algorithm selects the same number of sampling sites within each region in order to

443   maximize physical distance between sites. Increasing environmental variation is expected to

444   raise the sensitivity of seascape genomics analysis, while the replication of environmental

445   gradients is expected to reduce false discovery rates (Selmoni et al. 2020a). Here the number

446   of environmental clusters was five (Fig. S3) and we established at four sampling locations per

447   cluster. When this was not possible (*e.g.* because of logistic constraints during the sampling

448   campaign), additional sampling sites were added to the neighbouring clusters.

449 The sampling campaign was performed from February to May 2018 (under the permits

450 N°609011-/2018/DEPART/JJC and N°783-2018/ARR/DENV) and targeted three flagship

451 species of the Indo-Pacific: *Acropora millepora, Pocillopora damicornis sensu* Schmidt-Roach

452 et al. (2013) [corresponding to PSH04 *sensu* P. Gélin et al. (2017)] and *Pocillopora acuta sensu*

453 Schmidt-Roach et al. (2013) [corresponding to PSH05 *sensu* P. Gélin et al. (2017)]. Of note,

454 *P. acuta* and *P. damicornis* belong to the complex of species formerly named *P. damicornis*

455 (Schmidt-Roach et al. 2014; Johnston et al. 2017; Gélin, Fauvelot, et al. 2018). At every

456 sampling site, we collected up to 20 samples of *A. millepora* and 20 of *Pocillopora* aff.

457 *damicornis* (we did not discriminate between species while sampling as it can be difficult to

458 distinguish them in the field). All the samples were collected in a 1 km area and at a depth

459 ranging between 2-4 m. The centre of this area was used for georeferencing the sampling site.

460 Before sampling, each colony was imaged underwater, then a portion of a branch was

461 sampled with hammer and chisel. Each sample consisted of a 1-2 cm branch that was

462 immediately transferred to 80% ethanol and stored at -20°C. DNA from the 730 samples (370

463 *A. millepora* and 360 *Pocillopora;* Tab. S1) were extracted using the DNeasy 96 Tissue kit

464 (Qiagen) following manufacturer instructions.

465

466 Pocillopora *species identification*

467

468 The 360 *Pocillopora* samples were identified molecularly *a posteriori* of sampling to be

469 assigned to one species or the other (*P. damicornis or P. acuta*). Samples were thus genotyped

470 using 13 microsatellite loci, as in Gélin et al. (2017; Online Resource 1). Then, colonies

471 belonging to *P. damicornis* and to *P. acuta* were identified using assignment tests performed

472 with STRUCTURE (v. 2.3.4 ;Pritchard et al. 2000), as in Gélin et al. (2018). Colonies assigned to

473 *P. damicornis* or *acuta* with a probability of at least 0.70 were retained in the final dataset for

474 this study. The *Pocillopora* sampling was composed of 148 *P. damicornis* (more precisely to

475 SSH04b *sensu* Gélin et al. 2017), 159 *P. acuta* colonies (more precisely, a mix of SSH05a and

476 SSH05b *sensu* Gélin, Pirog, et al. 2018) and 53 unassigned colonies (excluded from further

477 analysis; Tab. S1).

478

479 Acropora *species identification*

480   *Acropora* species are genetically and morphologically notoriously challenging in terms of

481   identification and species boundaries detection. However, *A. millepora* can be recognised in

482   the field based on its typical axial and radial corallite shape (Wallace 1999).Back from the

483   field, *in situ* images of each specimen were examined to look for the species diagnostic

484   morphological characters and initial identifications validated.

485

486   *Screening and SNP genotyping*

487

488   All DNA samples from *A. millepora*, *P. damicornis* and *P. acuta* were sent to the Diversity

489   Arrays Technology (Canberra, Australia) for quality check screening and genotype-by-

490   sequencing using the DArT-sequencing method (DArT-seq; Kilian et al. 2012). The restriction

491   enzymes used for library preparation for *A. millepora* and *Pocillopora* samples were PstI and

492   HpaII. Prior to sequencing, all the DNA samples underwent a one-hour incubation with the

493   digestion buffer, followed by a step of quality check for integrity, purity and concentration

494   running 1 μL per sample on a 0.8% agarose gel. Samples from each site were then ranked

495   based on their quality (degree of smearing on the agarose gel). We then selected the samples

496   with the best scores from each site and defined a list of 188 *A. millepora,* 128 *P. damicornis*

497   and 150 *P. acuta* samples that proceeded to the sequencing step in four and five lanes of an

498   Illumina Hiseq2500, respectively. During each step of the workflow (DNA purification, library

499   preparation and sequencing), *A. millepora* and *Pocillopora* samples were kept separated and

500   randomly distributed across the respective batches (*e.g.* 96-well plates, sequencing lanes) to

501   minimize the risks of technical bias. SNPs were called using the DArT-seq analytical pipeline

502   (DArTsoft14).

503

504   *SNP filtering*

505

506   The DArT-loci (*i.e.* the DNA sequences surrounding each SNP) initially underwent a sequence

507   similarity search (BLASTn; v. 2.7.1; Madden and Coulouris 2008) against a reference genome

508   to retain only those associated with the coral host. For *A. millepora,* the reference genome

509   was the *A. millepora* chromosome-level assembly from Fuller and colleagues (v. 2; Fuller et

510   al. 2019, unpublished data, available on arXiv), while for *P. damicornis* and *P. acuta* we used

511   the only *Pocillopora* reference assembled to date (*P. damicornis sensu lato;* v. 1; Cunning et

512   al. 2018). Only DArT-loci scoring an E-value below 10^{-6} were retained.

513   The processing of the SNPs data followed a pipeline from previous work on coral seascape

514   genomics (Selmoni et al. 2020b). For each species' dataset, we removed SNPs and individuals

515   with high missing rates (> 50%) by using custom functions in the R environment. Next, we

516   proceeded with imputation of missing genotypes using the *linkimpute* algorithm (based on k-

517   nearest-neighbours imputation; Money et al. 2015) implemented in Tassel 5 (Bradbury et al.

518   2007) using the default settings. Afterwards, we repeated the filtering of SNPs and individuals

519   for missing rates, but this time using a more stringent threshold (5%). We also applied a filter

520   to exclude rare alleles (minor allele frequency < 5%) and highly frequent genotypes (major

521   genotype frequency > 95%). SNPs were then filtered for linkage disequilibrium using the R

522   package *SNPrelate* (function *snpsgdsLDpruning*, LDthreshold=0.3, v.1.16; Zheng et al. 2012).

523   Finally, we applied a filter for clonality: when groups of colonies shared highly correlated

524   genotypes (Pearson correlation > 0.9) only one colony pert group was kept.

525

526   *Neutral genetic structure analysis*

527

528   Prior to the seascape genomics analysis, the neutral genetic structure of the studied

529   populations was investigated by running a PCA on the genotype matrix of each species using

530   the R *stats* package (*prcomp* function). Firstly, we visually inspected the percentage of

531   variance of the genotype matrix explained by each principal component (eigenanalysis); in

532   highly structured populations the first principal components (PCs) are expected to explain a

533   larger proportion of the variance, when compared to the subsequent PCs (Johnstone 2001;

534   Novembre et al. 2008). We ran a Tracy-Widom test as implemented in R package *AssocTests*

535   (Wang et al. 2017) to determine the number of PCs underlying a non-random genetic

536   structure ($P < 0.05$; Patterson et al. 2006).

537   We also visualized the spatial distribution of the main axis of variation (PC1), in order to

538   investigate the presence of geographical structures (Novembre et al. 2008). Finally, we

539   focused on the SNP-specific loadings on PC1 and their distributions across the genome. In

540   fact, groups of genetically isolated individuals (*e.g.* hybrids, cryptic species) are expected to

541   display genomic islands of low-recombination (*i.e.* groups of physically close SNPs

542   contributing to high loading on the main axis of variation; Nosil et al. 2009; Li and Ralph 2019).

543   We therefore visualized the distribution of average PC1-loadings by genomic windows of 50

544   and 100 kb. In these calculations, only genomic windows containing at least 5 SNPs were

545   retained.

546

547   *Seascape genomics*

548

549   The seascape genomics analyses were performed separately on the three species using the

550   LFMM method implemented in the *LEA* R package (v. 2.4.0; Frichot et al. 2013; Frichot and

551   François 2015). This method associates single environmental gradients and individual SNPs

552   variations in mixed models, where the confounding effect of neutral genetic variation is

553   accounted for through latent factors (Frichot et al. 2013).

554   Briefly, the first step of the LFMM pipeline is to estimate the number of latent factors (K;

555   Frichot and François 2015). This parameter corresponds to the number of ancestral

556   populations and can be estimated by using the *snmf* function of the LEA package. The method

557   processes a genotype matrix to estimate individual admixture coefficients under different K's,

558   and then evaluates the quality of fit for each K via cross validation (Frichot and François 2015).

559   We ran ten replicates of this analysis for all the studied species, and found that the optimal

560   number of K (according to the lowest entropy criterion) ranged from 2-4 for *A. millepora,* 6-8

561   for *P. damicornis,* and 10-12 for *P. acuta* (Fig. S4).

562   We then proceeded to the genotype-environment association analysis with LFMM. Since this

563   method does not accept missing genotypes, we first ran the *impute* function of the LEA

564   package. For each species, this function inferred the missing genotypes out of the ancestral

565   genotype frequencies previously calculated with the *snmf* function. Finally, we ran the

566   association analysis between the SNPs of each species and the environmental condition

567   descriptors. This was done by using the *lfmm* function, setting K to the ranges previously

568   estimated for each species and running five replicates of each analysis. Since *lfmm*

569   calculations can be computationally intensive, when two or more environmental descriptors

570   were highly collinear (absolute value of Pearson correlation > 0.9), only one was used in the

571   analysis.

572   LFMM returns *P*-values describing the statistical significance of every genotype-environment

573   association under different values of K. For each association model related to the same

574   environmental variable, *P*-values were corrected for multiple testing using the q-value

575   method (R package *q-value*, v. 2.14, Storey 2003) and deemed significant if *q* < 0.01 under at

576   least one level of K. When a SNP was significantly associated to multiple environmental

577   variables, or with an environmental variable highly correlated with others (*i.e.* those excluded

578   from the LFMM calculations), we defined a main environmental descriptor as the variable

579   most strongly correlated (Pearson) with the SNP.

580

581   *Annotation analysis of heat stress associated SNPs*

582

583   For each of the three studied species, we annotated the genomic neighbourhood of every

584   SNP in order to characterize the possible functional implications of a genetic variant. Firstly,

585   we uniformed the annotations of genes from different species in order to facilitate

586   comparisons. We did this by retrieving the positions of genes in the two reference genomes

587   (Cunning et al. 2018; Fuller et al. 2019) and the corresponding predicted protein sequences.

588   These sequences were used to perform a similarity search (blastP; Madden and Coulouris

589   2008) against the Uniprot/swissprot database (*metazoa* entries, release 2020_01;

590   Boeckmann et al. 2003). Each gene was annotated with the best significant hit (E-value < 0.01)

591   and inherited protein name and gene ontology (GO) terms describing molecular functions

592   when existing (Ashburner et al. 2000).

593   Afterwards, we focused on the annotation of genes surrounding SNPs associated with heat

594   stress descriptors. Significant SNPs were deemed "heat stress associated" if they were best

595   correlated with an environmental descriptor relating to average temperature, standard

596   deviation of temperature, or bleaching alert frequency. We mapped every SNP associated

597   with heat stress as the genes located within a ± 50 kb window. We selected this window size

598   because genes associated with a SNP can be located hundreds of kilobases away (Visel et al.

599   2009; Brodie et al. 2016) , with 50 kb being roughly the median contig size in the *P. damicornis*

600   reference genome (Cunning et al. 2018).

601   We then computed the observed occurrence of each GO term among the genomic

602   neighbourhoods of significant SNPs. As a comparison, we split the reference genome into

603   100 kb windows and computed the expected occurrence for each term. This procedure was

604   performed separately for each of the three studied species, using the respective reference

605   genome. The statistical analysis of differences between the expected and observed GO term

606   occurrences (enrichment analysis) was performed using the Fisher exact test method as

25

607 implemented in the R *topGO* package (v. 2.34; Alexa et al. 2006). As suggested in the *topGO*

608 guidelines, we ranked GO terms according to the *P-value* of the Fisher test and discarded

609 those occurring fewer than 10 times throughout the genome.

610

611

Acknowledgments

613

621

622

References

624

625 Ahmad M, Srinivasula SM, Wang L, Talaniaii R V., Litwack G, Fernandes-Alnemri T, Alnemri
626 ES. 1997. CRADD, a novel human apoptotic adaptor molecule for caspase-2, and FasL/tumor
627 necrosis factor receptor-interacting protein RIP. Cancer Res. 57(4):615–619.

628 Alexa A, Rahnenführer J, Lengauer T. 2006. Improved scoring of functional groups from gene
629 expression data by decorrelating GO graph structure. Bioinformatics. 22(13):1600–1607.

630 Ashburner M, Ball CA, Blake JA, Botstein D, Butler H, Cherry JM, Davis AP, Dolinski K, Dwight
631 SS, Eppig JT, et al. 2000. Gene Ontology: Tool for The Unification of Biology. Nat Genet.
632 25(1):25–29.

633 Baums IB. 2008. A restoration genetics guide for coral reef conservation. Mol Ecol.
634 17(12):2796–2811.

635 Bay RA, Palumbi SR. 2014. Multilocus adaptation associated with heat resistance in reef-
636 building corals. Curr Biol. 24(24):2952–2956.

637 Bellwood DR, Hughes TP, Folke C, Nyström M. 2004. Confronting the coral reef crisis.
638 Nature. 429(6994):827–833.

639 Boeckmann B, Bairoch A, Apweiler R, Blatter MC, Estreicher A, Gasteiger E, Martin MJ,

640 Michoud K, O'Donovan C, Phan I, et al. 2003. The SWISS-PROT protein knowledgebase and
641 its supplement TrEMBL in 2003. Nucleic Acids Res. 31(1):365–370.

642 Bonesso JL, Leggat W, Ainsworth TD. 2017. Exposure to elevated sea-surface temperatures
643 below the bleaching threshold impairs coral recovery and regeneration following injury.
644 PeerJ. 2017(8).

645 Bradbury PJ, Zhang Z, Kroon DE, Casstevens TM, Ramdoss Y, Buckler ES. 2007. TASSEL:
646 Software for association mapping of complex traits in diverse samples. Bioinformatics.
647 23(19):2633–2635.

648 Brodie A, Azaria JR, Ofran Y. 2016. How far from the SNP may the causative genes be?
649 Nucleic Acids Res. 44(13):6046–54.

650 Chao Y, Li Z, Farrara JD, Hung P. 2009. Blending Sea Surface Temperatures from Multiple
651 Satellites and In Situ Observations for Coastal Oceans. J Atmos Ocean Technol. 26(7):1415–
652 1426.

653 Chin TM, Vazquez-Cuervo J, Armstrong EM. 2017. A multi-scale high-resolution analysis of
654 global sea surface temperature. Remote Sens Environ. 200:154–169.,

655 Courtial L, Picco V, Grover R, Cormerais Y, Rottier C, Labbe A, Pagès G, Ferrier-Pagès C. 2017.
656 The c-Jun N-terminal kinase prevents oxidative stress induced by UV and thermal stresses in
657 corals and human cells. Sci Rep. 7(1):45713.

658 Cunning R, Bay RA, Gillette P, Baker AC, Traylor-Knowles N. 2018. Comparative analysis of
659 the Pocillopora damicornis genome highlights role of immune system in coral evolution. Sci
660 Rep. 8(1):16134.

661 Dance A. 2019. These corals could survive climate change — and help save the world's reefs.
662 Nature. 575(7784):580–582.

663 Daniel DC, Dagdanova A V., Johnson EM. 2013. The MCM and RecQ Helicase Families:
664 Ancient Roles in DNA Replication and Genomic Stability Lead to Distinct Roles in Human
665 Disease. In: The Mechanisms of DNA Replication. InTech.

666 Darling ES, Alvarez-Filip L, Oliver TA, McClanahan TR, Côté IM. 2012. Evaluating life-history
667 strategies of reef corals from species traits. Bellwood D, editor. Ecol Lett. 15(12):1378–1386.

668 Desalvo MK, Sunagawa S, Voolstra CR, Medina M. 2010. Transcriptomic responses to heat
669 stress and bleaching in the elkhorn coral Acropora palmata. Mar Ecol Prog Ser. 402:97–113.

670 Desalvo MK, Voolstra CR, Sunagawa S, Schwarz JA, Stillman JH, Coffroth MA, Szmant AM,
671 Medina M. 2008. Differential gene expression during thermal stress and bleaching in the
672 Caribbean coral Montastraea faveolata. Mol Ecol. 17(17):3952–3971.

673 Dunn SR, Pernice M, Green K, Hoegh-Guldberg O, Dove SG. 2012. Thermal Stress Promotes
674 Host Mitochondrial Degradation in Symbiotic Cnidarians: Are the Batteries of the Reef Going
675 to Run Out? Polymenis M, editor. PLoS One. 7(7):e39024.

676   Dunn SR, Schnitzler CE, Weis VM. 2007. Apoptosis and autophagy as mechanisms of
677   dinoflagellate symbiont release during cnidarian bleaching: Every which way you lose. Proc
678   R Soc B Biol Sci. 274(1629):3079–3085.

679   EU Copernicus Marine Service. 2017. Global Ocean - In-Situ-Near-Real-Time Observations.

680   Frichot E, François O. 2015. LEA: An R package for landscape and ecological association
681   studies. O'Meara B, editor. Methods Ecol Evol. 6(8):925–929.

682   Frichot E, Schoville SD, Bouchard G, François O. 2013. Testing for associations between loci
683   and environmental gradients using latent factor mixed models. Mol Biol Evol. 30(7):1687–
684   1699.

685   Fuller ZL, Mocellin VJL, Morris L, Cantin N, Shepherd J, Sarre L, Peng J, Liao Y, Pickrell J,
686   Andolfatto P, et al. 2019. Population genetics of the coral Acropora millepora: Towards a
687   genomic predictor of bleaching. bioRxiv.:867754.
688   https://www.biorxiv.org/content/10.1101/867754v1, last accessed 24-02-20

689   Gélin P, Fauvelot C, Bigot L, Baly J, Magalon H. 2018. From population connectivity to the art
690   of striping Russian dolls: the lessons from *Pocillopora* corals. Ecol Evol. 8(2):1411–1426.

691   Gélin P, Pirog A, Fauvelot C, Magalon H. 2018. High genetic differentiation and low
692   connectivity in the coral Pocillopora damicornis type β at different spatial scales in the
693   Southwestern Indian Ocean and the Tropical Southwestern Pacific. Mar Biol. 165(10).

694   Gélin P, Postaire B, Fauvelot C, Magalon H. 2017. Reevaluating species number, distribution
695   and endemism of the coral genus Pocillopora Lamarck, 1816 using species delimitation
696   methods and microsatellites. Mol Phylogenet Evol. 109:430–446.

697   Henry MD, Yancey SD, Kushner SR. 1992. Role of the heat shock response in stability of
698   mRNA in Escherichia coli K-12. J Bacteriol. 174(3):743–748.

699   Hijmans RJ. 2016. raster: Geographic Data Analysis and Modeling.

700   Van Hooidonk R, Maynard JA, Planes S. 2013. Temporary refugia for coral reefs in a warming
701   world. Nat Clim Chang. 3(5):508–511.

702   Hughes TP, Kerry JT, Álvarez-Noriega M, Álvarez-Romero JG, Anderson KD, Baird AH,
703   Babcock RC, Beger M, Bellwood DR, Berkelmans R, et al. 2017. Global warming and
704   recurrent mass bleaching of corals. Nature. 543(7645):373–377.

705   Hughes TP, Kerry JT, Baird AH, Connolly SR, Dietzel A, Eakin CM, Heron SF, Hoey AS,
706   Hoogenboom MO, Liu G, et al. 2018. Global warming transforms coral reef assemblages.
707   Nature. 556(7702):492–496.

708   Hughes TP, Kerry JT, Connolly SR, Baird AH, Eakin CM, Heron SF, Hoey AS, Hoogenboom MO,
709   Jacobson M, Liu G, et al. 2019. Ecological memory modifies the cumulative impact of
710   recurrent climate extremes. Nat Clim Chang. 9(1):40–43.

711   Ishikawa Y, Wirz J, Vranka JA, Nagata K, Bächinger HP. 2009. Biochemical characterization of

712   the prolyl 3-hydroxylase 1·Cartilage-associated protein·cyclophilin B complex. J Biol Chem.
713   284(26):17641–17647.

714   Johnston EC, Forsman ZH, Flot JF, Schmidt-Roach S, Pinzón JH, Knapp ISS, Toonen RJ. 2017. A
715   genomic glance through the fog of plasticity and diversification in Pocillopora. Sci Rep.
716   7(1):1–11.

717   Johnstone IM. 2001. On the Distribution of the Largest Eigenvalue in Principal Components
718   Analysis. Ann Stat. 29(2):295–327.

719   Kilian A, Wenzl P, Huttner E, Carling J, Xia L, Blois H, Caig V, Heller-Uszynska K, Jaccoud D,
720   Hopper C, et al. 2012. Diversity arrays technology: A generic genome profiling technology on
721   open platforms. Methods Mol Biol. 888:67–89.

722   Krueger T, Horwitz N, Bodin J, Giovani ME, Escrig S, Meibom A, Fine M. 2017. Common reef-
723   building coral in the northern red sea resistant to elevated temperature and acidification. R
724   Soc Open Sci. 4(5):170038.

725   Kültz D. 2005. Molecular and Evolutionary Basis of the Cellular Stress Response. Annu Rev
726   Physiol. 67(1):225–257.

727   Lee K, Tong LT, Millero FJ, Sabine CL, Dickson AG, Goyet C, Park G-H, Wanninkhof R, Feely
728   RA, Key RM. 2006. Global relationships of total alkalinity with salinity and temperature in
729   surface waters of the world's oceans. Geophys Res Lett. 33(19):L19605.

730   Leempoel K, Duruz S, Rochat E, Widmer I, Orozco-terWengel P, Joost S. 2017. Simple Rules
731   for an Efficient Use of Geographic Information Systems in Molecular Ecology. Front Ecol
732   Evol. 5:33.

733   Li H, Ralph P. 2019. Local PCA shows how the effect of population structure differs along the
734   genome. Genetics. 211(1):289–304.

735   Li J, Wang QE, Zhu Q, El-Mahdy MA, Wani G, Prætorius-Ibba M, Wani AA. 2006. DNA
736   damage binding protein component DDB1 participates in nucleotide excision repair through
737   DDB2 DNA-binding and cullin 4a ubiquitin ligase activity. Cancer Res. 66(17):8590–8597.

738   Liu G, Strong AE, Skirving W. 2003. Remote sensing of sea surface temperatures during 2002
739   Barrier Reef coral bleaching. Eos, Trans Am Geophys Union. 84(15):137–141.

740   Logan CA, Dunne JP, Eakin CM, Donner SD. 2014. Incorporating adaptive responses into
741   future projections of coral bleaching. Glob Chang Biol. 20(1):125–139.

742   Louis YD, Bhagooli R, Kenkel CD, Baker AC, Dyall SD. 2017. Gene expression biomarkers of
743   heat stress in scleractinian corals: Promises and limitations. Comp Biochem Physiol Part - C
744   Toxicol Pharmacol. 191:63–77.

745   Loya Y, Sakai K, Yamazato K, Nakano Y, Sambali H, van Woesik R. 2001. Coral bleaching: the
746   winners and the losers. Ecol Lett. 4(2):122–131.

747   Lutz A, Raina JB, Motti CA, Miller DJ, Van Oppen MJH. 2015. Host coenzyme Q redox state is

748   an early biomarker of thermal stress in the coral Acropora millepora. PLoS One.
749   10(10):e0139290.

750   Madden T, Coulouris G. 2008. BLAST Command Line Applications User Manual BLAST
751   Command Line Applications User Manual - BLAST ® ... (Md):1–28.

752   Maor-Landaw K, Karako-Lampert S, Ben-Asher HW, Goffredo S, Falini G, Dubinsky Z, Levy O.
753   2014. Gene expression profiles during short-term heat stress in the red sea coral Stylophora
754   pistillata. Glob Chang Biol. 20(10):3026–3035.

755   Maor-Landaw K, Levy O. 2016. Gene expression profiles during short-term heat stress;
756   branching vs. massive Scleractinian corals of the Red Sea. PeerJ. 2016(3).

757   Mason NJ, Fiore J, Kobayashi T, Masek KS, Choi Y, Hunter CA. 2004. TRAF6-dependent
758   mitogen-activated protein kinase activation differentially regulates the production of
759   interleukin-12 by macrophages in response to Toxoplasma gondii. Infect Immun.
760   72(10):5662–5667.

761   Matz M V., Treml EA, Aglyamova G V., Bay LK. 2018. Potential and limits for rapid genetic
762   adaptation to warming in a Great Barrier Reef coral. Hoekstra HE, editor. PLoS Genet.
763   14(4):e1007220.

764   Money D, Gardner K, Migicovsky Z, Schwaninger H, Zhong GY, Myles S. 2015. LinkImpute:
765   Fast and accurate genotype imputation for nonmodel organisms. G3 Genes, Genomes,
766   Genet. 5(11):2383–2390.

767   Muñoz-Gómez SA, Slamovits CH, Dacks JB, Wideman JG. 2015. The evolution of MICOS:
768   Ancestral and derived functions and interactions. Commun Integr Biol. 8(6):1–5.

769   Mydlarz LD, McGinty ES, Harvell CD. 2010. What are the physiological and immunological
770   responses of coral to climate warming and disease? J Exp Biol. 213(6):934–45.

771   Nielsen DA, Petrou K, Gates RD. 2018. Coral bleaching from a single cell perspective. ISME J.
772   12(6):1558–1567.

773   Nosil P, Funk DJ, Ortiz-Barrientos D. 2009. Divergent selection and heterogeneous genomic
774   divergence. Mol Ecol. 18(3):375–402.

775   Novembre J, Johnson T, Bryc K, Kutalik Z, Boyko AR, Auton A, Indap A, King KS, Bergmann S,
776   Nelson MR, et al. 2008. Genes mirror geography within Europe. Nature. 456(7218):98–101.

777   Oakley CA, Durand E, Wilkinson SP, Peng L, Weis VM, Grossman AR, Davy SK. 2017. Thermal
778   Shock Induces Host Proteostasis Disruption and Endoplasmic Reticulum Stress in the Model
779   Symbiotic Cnidarian Aiptasia. J Proteome Res. 16(6):2121–2134.

780   van Oppen MJH, Gates RD, Blackall LL, Cantin N, Chakravarti LJ, Chan WY, Cormick C, Crean
781   A, Damjanovic K, Epstein H, et al. 2017. Shifting paradigms in restoration of the world's coral
782   reefs. Glob Chang Biol. 23(9):3437–3448.

783   van Oppen MJH, Lough JM. 2009. Coral Bleaching — Patterns, Processes, Causes and

784   Consequences. Springer. p. 298–201.

785   Van Oppen MJH, Oliver JK, Putnam HM, Gates RD. 2015. Building coral reef resilience
786   through assisted evolution. Proc Natl Acad Sci U S A. 112(8):2307–2313.

787   Palumbi SR, Barshis DJ, Traylor-Knowles N, Bay RA. 2014. Mechanisms of reef coral
788   resistance to future climate change. Science (80-). 344(6186).

789   Patel R, Rinker L, Peng J, Chilian WM. 2018. Reactive Oxygen Species: The Good and the Bad.
790   In: Reactive Oxygen Species (ROS) in Living Cells. InTech.

791   Patterson N, Price AL, Reich D. 2006. Population structure and eigenanalysis. PLoS Genet.
792   2(12):2074–2093.

793   Penin L, Vidal-Dupiol J, Adjeroud M. 2013. Response of coral assemblages to thermal stress:
794   are bleaching intensity and spatial patterns consistent between events? Environ Monit
795   Assess. 185(6):5031–5042.

796   Porté S, Valencia E, Yakovtseva EA, Borràs E, Shafqat N, Debreczeny JE, Pike ACW,
797   Opperman U, Farrés J, Fita I, et al. 2009. Three-dimensional structure and enzymatic
798   function of proapoptotic human p53-inducible quinone oxidoreductase PIG3. J Biol Chem.
799   284(25):17194–17205.

800   Prindle MJ, Loeb LA. 2012. DNA polymerase delta in dna replication and genome
801   maintenance. Environ Mol Mutagen. 53(9):666–682.

802   Pritchard JK, Stephens M, Donnelly P. 2000. Inference of population structure using
803   multilocus genotype data. Genetics. 155(2):945–959.

804   QGIS development team. 2009. QGIS Geographic Information System. Open Source
805   Geospatial Foundation Project.

806   R Core Team. 2016. R: A Language and Environment for Statistical Computing.

807   Rellstab C, Gugerli F, Eckert AJ, Hancock AM, Holderegger R. 2015. A practical guide to
808   environmental association analysis in landscape genomics. Mol Ecol. 24(17):4348–4370.

809   Ren B, Liu M, Ni J, Tian J. 2018. Role of selenoprotein f in protein folding and secretion:
810   Potential involvement in human disease. Nutrients. 10(11).

811   Ricaurte M, Schizas N V., Ciborowski P, Boukli NM. 2016. Proteomic analysis of bleached and
812   unbleached Acropora palmata, a threatened coral species of the Caribbean. Mar Pollut Bull.
813   107(1):224–232.

814   Riginos C, Crandall ED, Liggins L, Bongaerts P, Treml EA. 2016. Navigating the currents of
815   seascape genomics: how spatial analyses can augment population genomic studies. Curr
816   Zool. 62:doi: 10.1093/cz/zow067.

817   Roche RC, Williams GJ, Turner JR. 2018. Towards Developing a Mechanistic Understanding
818   of Coral Reef Resilience to Thermal Stress Across Multiple Scales. Curr Clim Chang Reports.

819   4(1):51–64.

820   Rosic NN, Pernice M, Dove S, Dunn S, Hoegh-Guldberg O. 2011. Gene expression profiles of
821   cytosolic heat shock proteins Hsp70 and Hsp90 from symbiotic dinoflagellates in response
822   to thermal stress: Possible implications for coral bleaching. Cell Stress Chaperones.
823   16(1):69–80.

824   Ruiz-Jones LJ, Palumbi SR. 2017. Tidal heat pulses on a reef trigger a fine-tuned
825   transcriptional response in corals to maintain homeostasis. Sci Adv. 3(3):e1601298.

826   Safaie A, Silbiger NJ, McClanahan TR, Pawlak G, Barshis DJ, Hench JL, Rogers JS, Williams GJ,
827   Davis KA. 2018. High frequency temperature variability reduces the risk of coral bleaching.
828   Nat Commun. 9(1).

829   Schmidt-Roach S, Lundgren P, Miller KJ, Gerlach G, Noreen AME, Andreakis N. 2013.
830   Assessing hidden species diversity in the coral Pocillopora damicornis from Eastern
831   Australia. Coral Reefs. 32(1):161–172.

832   Schmidt-Roach S, Miller KJ, Lundgren P, Andreakis N. 2014. With eyes wide open: a revision
833   of species within and closely related to the *Pocillopora damicornis* species complex
834   (Scleractinia; Pocilloporidae) using morphology and genetics. Zool J Linn Soc. 170(1):1–33.

835   Selmoni O, Vajana E, Guillaume A, Rochat E, Joost S. 2020a. Sampling strategy optimization
836   to increase statistical power in landscape genomics: A simulation-based approach. Mol Ecol
837   Resour. 20(1).

838   Selmoni O, Rochat E, Lecellier G, Berteaux-Lecellier V, Joost S. 2020b. Seascape genomics as
839   a new tool to empower coral reef conservation strategies: an example on north-western
840   Pacific Acropora digitifera. Evol Appl.:588228.

841   Sharma S, Doherty KM, Brosh RM, Jr. 2006. Mechanisms of RecQ helicases in pathways of
842   DNA metabolism and maintenance of genomic stability. Biochem J. 398(3):319–37.

843   Smits VAJ, Cabrera E, Freire R, Gillespie DA. 2019. Claspin – checkpoint adaptor and DNA
844   replication factor. FEBS J. 286(3):441–455.

845   Son Y, Kim S, Chung HT, Pae HO. 2013. Reactive oxygen species in the activation of MAP
846   kinases. In: Methods in Enzymology. Vol. 528. Academic Press Inc. p. 27–48.

847   Sottile ML, Nadin SB. 2018. Heat shock proteins and DNA repair mechanisms: an updated
848   overview. Cell Stress Chaperones. 23(3):303–315.

849   Storey JD. 2003. The Positive False Discovery Rate: A Bayesian Interpretation and the q-
850   Value. Ann Stat. 31(6):2013–2035.

851   Sully S, Burkepile DE, Donovan MK, Hodgson G, van Woesik R. 2019. A global analysis of
852   coral bleaching over the past two decades. Nat Commun. 10(1):1–5.

853   Tchernov D, Kvitt H, Haramaty L, Bibbyd TS, Gorbunov MY, Rosenfeld H, Falkowski PG. 2011.
854   Apoptosis and the selective survival of host animals following thermal bleaching in

855   zooxanthellate corals. Proc Natl Acad Sci U S A. 108(24):9905–9909.

856   Thomas L, Kennington WJ, Evans RD, Kendrick GA, Stat M. 2017. Restricted gene flow and
857   local adaptation highlight the vulnerability of high-latitude reefs to rapid environmental
858   change. Glob Chang Biol. 23(6):2197–2205.

859   Thompson DM, van Woesik R. 2009. Corals escape bleaching in regions that recently and
860   historically experienced frequent thermal stress. Proc Biol Sci. 276(1669):2893–2901.

861   UNEP-WCMC, WorldFish-Center, WRI, TNC. 2010. Global distribution of warm-water coral
862   reefs, compiled from multiple sources including the Millennium Coral Reef Mapping Project.
863   Version 1.3.

864   Valmiki MG, Ramos JW. 2009. Death effector domain-containing proteins. Cell Mol Life Sci.
865   66(5):814–830.

866   Visel A, Rubin EM, Pennacchio LA. 2009. Genomic views of distant-acting enhancers. Nature.
867   461(7261):199–205.

868   Voolstra CR, Schnetzer J, Peshkin L, Randall CJ, Szmant AM, Medina M. 2009. Effects of
869   temperature on gene expression in embryos of the coral Montastraea faveolata. BMC
870   Genomics. 10:627.

871   Voolstra CR, Sunagawa S, Matz M V., Bayer T, Aranda M, Buschiazzo E, DeSalvo MK,
872   Lindquist E, Szmant AM, Coffroth MA, et al. 2011. Rapid evolution of coral proteins
873   responsible for interaction with the environment. PLoS One. 6(5).

874   Wallace CC. 1999. Staghorn corals of the world : a revision of the coral genus Acropora
875   (Scleractinia ; Astrocoeniina ; Acroporidae) worldwide, with emphasis on morphology,
876   phylogeny and biogeography. CSIRO.

877   Wang L, Zhang W, Li Q, Zhu W. 2017. AssocTests: Genetic Association Studies.

878   Wilson C, Terman JR, González-Billault C, Ahmed G. 2016. Actin filaments—A target for
879   redox regulation. Cytoskeleton. 73(10):577–595.

880   Yuasa K, Ota R, Matsuda S, Isshiki K, Inoue M, Tsuji A. 2015. Suppression of death-associated
881   protein kinase 2 by interaction with 14-3-3 proteins. Biochem Biophys Res Commun.
882   464(1):70–75.

883   Zangar RC, Davydov DR, Verma S. 2004. Mechanisms that regulate production of reactive
884   oxygen species by cytochrome P450. Toxicol Appl Pharmacol. 199(3):316–331.

885   Zhao RZ, Jiang S, Zhang L, Yu Z Bin. 2019. Mitochondrial electron transport chain, ROS
886   generation and uncoupling (Review). Int J Mol Med. 44(1):3–15.

887   Zheng M, Cierpicki T, Burdette AJ, Utepbergenov D, Janczyk PL, Derewenda U, Stukenberg
888   PT, Caldwell KA, Derewenda ZS. 2011. Structural features and chaperone activity of the
889   NudC protein family. J Mol Biol. 409(5):722–741.

890   Zheng X, Levine D, Shen J, Gogarten SM, Laurie C, Weir BS. 2012. A high-performance
891   computing toolset for relatedness and principal component analysis of SNP data.
892   Bioinformatics. 28(24):3326–3328.

893